Compositional Changes During the Wet Spinning of Acrylic Fibers from Aqueous Sodium Thiocyanate Solvent

S. J. LAW, S. K. MUKHOPADHYAY

Department of Textile Industries, University of Leeds, Leeds LS2 9JT, United Kingdom

Received 10 July 1997; accepted 21 November 1997

ABSTRACT: The compositional changes taking place during the wet spinning of acrylic fibers from an aqueous sodium thiocyanate solvent were investigated. The composition of the fibers diverted from the precipitation bath after various immersion times was determined gravimetrically, while fiber diameters were imaged to ascertain volumetric changes with time. The kinetics of phase separation were approximated using light transmission and video techniques applied to acrylic films. For coagulation into water at 20 and 40°C and into 15% aqueous NaSCN at 20°C, a greater influx of the nonsolvent to outflow of the solvent was recorded at short timescales. Unexpectedly, both the outflow of the solvent and nonsolvent against the concentration gradient was noted at longer timescales, suggested by the light transmission data to be after the primary phase separation. The consequent reduction in filament diameter, hence, the volume, is discussed in terms of a coarsening mechanism, whereby the mobile polymer lean phase has a route away from the filament into the bath during polymer coarsening. Finally, the compositional changes are plotted on a phase diagram for the system as trajectories into the two-phase region. The polymer-coarsening effect renders the interpretation at longer timescales uncertain. © 1998 John Wiley & Sons, Inc. J Appl Polym Sci 69: 1459–1469, 1998

INTRODUCTION

In a recent publication,[1] the construction of a phase diagram for the commercially important ternary system polyacrylonitrile (PAN)/sodium thiocyanate (NaSCN)/water, used to wet spin acrylic fibres, was described. During precipitation of the filament extrudate, it was assumed that the sodium thiocyanate (solvent) was diffusing out of the filament, while water (nonsolvent) was diffusing into it. The composition of the single-phase solution thereby was changing gradually until the binodal was traversed and the system entered the unstable two-phase region of the composition diagram. It is thus important to know a fairly precise location of the limit of stability as a function of the concentration of the three components. Of equal importance is the trajectory into the two-phase region taken by the precipitating filament. For instance, the polymer concentration at which the binodal is crossed tends to dictate the nature of the recovered solid phase; traversing the binodal at a polymer concentration above or below the critical point dictates whether it is the polymer-rich phase or the polymer-depleted phase, respectively, which forms the continuous phase with integrity. Furthermore, the rate of the composition change can dictate the disposition of the two newly formed phases through the rate of growth processes (nucleation and growth or spinodal decomposition) before "solidification" arrests the process.

The geometry and dynamics of a nascent spinning filament in a precipitation bath makes inves-

Correspondence to: S. K. Mukhopadhyay.

Journal of Applied Polymer Science, Vol. 69, 1459–1469 (1998)
 CCC 0021-8995/98/071459-11

tigation of the compositional change and its associated kinetics very difficult. In cast membrane geometry, the task is somewhat simplified. In this case, a flat sheet can be held motionless while the exchange processes are studied. Such studies have been undertaken extensively in the membrane field and have been reviewed by Mulder.[2] In this article, both fiber and membrane forms are utilized in a complimentary fashion to study the magnitude and rate of compositional change of an acrylic wet spinning system based on the PAN copolymer in sodium thiocyanate/water and to relate these to the previously determined phase diagram.[1]

EXPERIMENTAL

The kinetic studies of polymer precipitation were based on a 13% by weight solution of a poly(acrylonitrile-*co*-methylacrylate-*co*-sulfonic acid) polymer, typical of a commercial acrylic fiber composition, in a 56.8% w/w aqueous sodium thiocyanate solvent.

Determination of the Kinetics of Phase Separation

Light Transmission Technique

When a polymer solution is immersed into a nonsolvent environment to spin fibers or to cast membranes, solvent and nonsolvent exchange takes place. At some point through the thickness of the membrane or filament, a composition is reached which lies at the point of instability and phase separation begins to take place. At high polymer concentrations (usually above 5%), a polymer lean phase grows while a polymer-rich phase is created. The discontinuities created, depending on their size and density difference, can become visible to the eye as the film becomes opaque. This effect can be used to study the onset and progression of phase separation through the polymer solution film. Experiments exploiting this phenomenon were described by Reuvers and Smolders.[3]

A glass dish was placed on a block of wood 2-in. thick, through which a channel was drilled at the center. At the base of the channel, an eye-response photodiode was carefully glued so that the photodiode element faced upward through the channel. The signal from the photodiode was amplified by a custom-built op amp circuit. The amplified signal was then fed to a chart recorder. A microscope lamp was suspended above the wooden block, positioned such that it illuminated the channel drilled at the center.

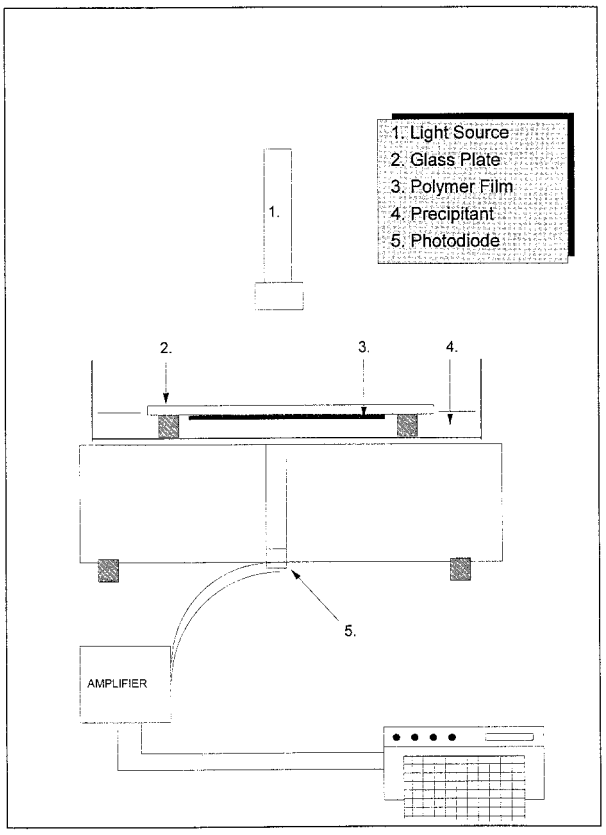

Figure 1 Schematic diagram of light transmission unit.

In a typical experiment, a film of the polymer solution is prepared in the conventional way by drawing a smooth casting bar fitted with wire spacers of the appropriate diameter for the film thickness required over a small pool of solution. The glass plate is then inverted and placed onto four supporting rubber bungs in the glass dish so that the film is underneath the plate (see Fig. 1). The precipitant is then poured carefully into the dish, not quite up to the film. At this point, the intensity of the lamp is adjusted to give about 80% of full scale on the chart recorder. The recorder drive is then started and the dish further filled until the film is just covered, but not the glass plate. In this way, stray reflections from an air/liquid interface which make the data noisy are eliminated. When phase separation sets in, a decrease in light intensity is measured by the chart recorder as a function of time, as the film becomes opaque.

Precipitations were carried out in water at 20 and 40°C and in 15% NaSCN at 20°C. For experi-

ments at elevated temperature, a dish covered in an expanded polystyrene sheet was used. The thermal mass of the precipitant and dish was sufficient so as to make temperature control unnecessary.

Video Technique

The light transmission technique described above can suffer a low signal-to-noise ratio, as the refractive index changes due to the egressing solvent passing the light path can mask changes due to the changing film opacity. This is particularly true for films which are very thin and for which the total light attenuation on phase separation is small.

Consequently, an alternative technique was developed for this study, which is based on video photography. The arrangement of the coagulating film is as described above for the light transmission technique, but, importantly, the precipitation dish was placed on a matt black surface. The changing clarity of the polymer film was monitored directly using a video camera (Sony V6000) equipped with a wide-angle lens (Sigma). Each coagulation experiment was thus recorded into a digital edit suite (FAST Electronic GmbH) at a rate of one frame per 40 ms. Each frame was then converted to a PC graphics file (8 bit) and analyzed using Optimas 5.2 software (Optimas Corp.). This software allowed random points to be chosen (20 taken) on the polymer film which could be assigned a gray scale number, depending on how the clarity of the coagulating film increased the value of the black background. The 8-bit nature of the graphic image gave a resolution of 256 shades from black to white, which was found to give sufficient resolution for the 64-μm films measured using this technique. Measurements were carried out at the three precipitation conditions described previously.

Determination of Compositional Change

During a dynamic single-filament spinning experiment, the average composition at any distance from the spinneret face through the precipitation bath can be determined by leading the filament out of the bath at a given point, collecting it, and analyzing it for the overall composition. As an additional check, the diameter of the filament can be measured to ascertain the level of ingress or egress of the liquid due to the diffusion process.

Fiber Spinning

A polymer solution contained in a 1-in. outer diameter stainless-steel tube was forced by pressurized nitrogen through a single-hole spinneret with a hole diameter of 70 μm. A flow rate of 0.11 g/min was used, corresponding to a hypothetical final decitex of 3.3 following stretching to a ratio of 8 and a final speed of 40 m/min. In these circumstances, commercial extrusion conditions are approximated. The spinneret was immersed in a plastic bath filled with the precipitant, and collection of the coagulated filament was onto a roll unit set at a 5 m/min linear speed.

Measurement of Extruding Filament Diameter

The measurement of the filament diameter was carried out in real time using a photomicrographic method. A fiber optic endoscope (Moritex Scopeman 504) equipped with a $\times$210 objective was clamped into a 3-dimensional micropositioner (Beck) over the top of the filament. The output image was recorded onto a video recorder (Mitsubishi HS B11) with a good freeze-frame capability. In this way, images were recorded onto tape for examination at a later date. For the calibration of length scales, a 1-mm graticule was imaged with the endoscope and recorded and a conversion factor established for measurements taken from a TV screen.

Evaluation of Extruding Filament Composition

The single filament was guided out of the bath at different distances from the spinneret by a rotating collection roll and collected for about 30 s. Because of the single-filament nature and the relatively slow speed of collection, it was assumed that excess bath liquor was not carried over on the surface of the filament. The fiber bundle was quickly cut from the roller and weighed. The bundle was then dried in an oven at 80°C to remove water and again weighed. Finally, the fiber/solvent bundle was boil washed in water for 2 h to remove the solvent and weighed a final time. The reproducibility of the results for two separate fiber collections was found to be very good, with duplicate measurements within 4%. The composition of the original spinning dope was analyzed by casting approximately 100-μm-thick films and determining the components gravimetrically in a similar way.

Table I Composition of Filament as a Function of Precipitation Time in Water at 20°C

Coagulation Time (s)	Wt % PAN	Wt % NaSCN	Wt % Water	Ratio NaSCN : PAN	Ratio Water : PAN
0	12.8	49.5	37.7	3.87	2.95
0.12	11.9	42.8	45.3	3.60	3.81
0.18	12.2	42.0	45.9	3.44	3.76
0.30	12.8	38.3	49.0	2.99	3.83
1.08	13.8	29.4	56.8	2.13	4.12
2.46	15.6	18.4	66.0	1.18	4.23
10.20	23.5	1.3	75.2	0.06	3.2

RESULTS AND DISCUSSION

Compositional Change During Coagulation

In Table I, the changing composition of the coagulating filament is expressed as a function of time, computed from the distance traveled from the spinneret face, for precipitation into water at 20°C. The shortest timescale (120 ms) represents the shortest immersion distance at which continuous spinning was possible under these conditions.

The diffusional exchange process between the solvent and the nonsolvent is reflected in the relative amounts of these components as a function of time. Of significance is the concentration of the polymer in the phase-separated structure with time. Initially, the value decreases, suggesting a greater influx of nonsolvent than solvent egress. However, after about 120 ms, the situation is seemingly reversed as the polymer concentration increases, suggesting greater outflow of the solvent than ingress of the nonsolvent at that point. It is instructive to look at the ratios of water to PAN and of NaSCN to PAN shown in the last two columns of Table I. It is appropriate to assume that there is no diffusion of the polymer out of the nascent filament and that stretching of the extrudate has already taken place close to the spinneret where the fluid is the least viscous, so the respective ratios give an indication of the absolute amount of water and solvent, respectively, contained within the filament at any given time. It is clear that the solvent leaves the precipitating filament in a monotonic fashion. Of interest though is the behavior of the nonsolvent, which appears to enter very quickly for 2.5 s, but has left the filament in almost as great a quantity by just over 10 s. This is unusual and unexpected since there is still a concentration gradient across the filament boundary favoring *inflow* of the nonsolvent. For both the solvent and nonsolvent to diffuse from the filament at these later timescales, a volume contraction must take place.

Equivalent results are shown in Table II for precipitation into water at 40°C. An identical trend is observed at the higher temperature with regard to the outflow of the solvent and the inflow of the nonsolvent over short timescales, followed by an outflow of water (along with the solvent) later in the precipitation process.

Table III shows similar data for the precipitation into 15% aqueous sodium thiocyanate at 20°C. Once again, it can be seen that the solvent leaves the forming filament consistently, while, initially, the nonsolvent enters the filament at short timescales, but then later leaves, in this case significantly earlier than in the precipitation into water case.

Filament Diameter Change During Coagulation

From the video footage of the spinning filament, it was possible to measure diameters over a wide range of immersion distances—hence, precipitation times. Figure 2 shows the changing diameter of a nascent filament coagulating in water and in 15% sodium thiocyanate at 20°C and water at 40°C, up to a distance of 50 mm from the spinneret face, representing 600 ms. Due to the viscoelastic nature of the polymer solution, a significant die swell associated with the relief of normal stresses is evident. The point of maximum die swell was found to be about 70 μm from the die face. This diameter is plotted as the first point, not as the spinneret hole diameter of 70 μm, with subsequent points as a percentage of this initial diameter. Beyond the die swell, a fairly significant and rapid expansion of the filament occurs, being apparently greater in magnitude for precipitation into the pure nonsolvent. This is in reasonable agreement with the measured compositional

Table II Composition of Filament as a Function of Precipitation Time in Water at 40°C

Coagulation Time (s)	Wt % PAN	Wt % NaSCN	Wt % Water	Ratio NaSCN : PAN	Ratio Water : PAN
0	12.8	49.5	37.7	3.87	2.95
0.18	12.9	42.1	45.0	3.26	3.50
0.36	12.7	38.2	49.1	3.01	3.87
0.72	13.8	33.8	52.4	2.45	3.80
1.44	16.0	22.4	61.7	1.40	3.86
3.84	18.0	9.8	72.2	0.54	4.01
9.60	20.3	2.6	77.1	0.13	3.80

changes, which showed an increased level of nonsolvent inflow to solvent outflow at these short timescales.

Figure 3 shows the precipitation timescale extended to about 10 s with a dramatic change in the filament diameter. Beyond about 5 cm, representing 600-ms, the filament diameter falls fairly rapidly for precipitation at 20°C, approaching a constant diameter after 10 s, which is lower than the original die swollen extrudate. Again, this is qualitatively consistent with the compositional data, although the magnitude of the changes and exact timing do not coincide in each case. For instance, the swelling of filaments at short timescales is consistent with volume increases between 1.5 and 2.5 times. Whatever the relative fluxes of water and sodium thiocyanate during this time, the polymer concentration must be reduced to between 5.2 and 8.7% on an equal density basis. Even taking into account the fact that the density of sodium thiocyanate is likely to be greater than that of water (a 52% aqueous solution has a density of 1300 kg/m^3), the composition of the filament should be considerably lower, around 6–9%. Similarly, the contraction of the diameter at longer timescales is too small to account for the observed polymer concentrations of around 20% in this region. These anomalies appear to be attributable to experimental error. However, that the filament diameter first increases, then decreases, is indisputable.

The increase in diameter has already been explained in terms of a greater influx of water to an outflow of solvent. The reduction in diameter at longer timescales is more difficult to reconcile in simple diffusional terms. Coarsening of the just formed two-phase structure is a possible explanation. Structural coarsening was reported by McMaster[4] for polymer blends phase-separated by both nucleation and growth and spinodal decomposition, while others[5,6] considered coarsening in the thermal demixing of a polymer/solvent system. Such coarsening occurs to minimize the surface and so reduces the energy. Of the two possible mechanisms thought to operate, Ostwald ripening occurs for dispersed-phase structures, while interconnected structures coarsen through a viscous flow mechanism driven by interfacial tension. An exception was found by Aubert[7] for thermal quenches of polystyrene in cyclohexane, which, although bicontinuous, was observed to coarsen by a diffusive mechanism. A high viscosity of the polymer-rich phase rendering an extremely slow flow in favor of the diffusion of the polymer through the solvent-rich phase was offered as an explanation.

Where the separated structure is confined in

Table III Composition of Filament as Function of Precipitation Time in 15% NaSCN at 20°C

Coagulation Time (s)	Wt % PAN	Wt % NaSCN	Wt % Water	Ratio NaSCN : PAN	Ratio Water : PAN
0	12.8	49.5	37.7	3.87	2.95
0.30	11.5	39.4	49.1	3.43	4.27
0.36	12.5	40.0	47.5	3.20	3.80
1.44	15.0	30.9	54.1	2.06	3.61
2.28	16.3	24.4	59.3	1.50	3.64
9.96	19.7	17.4	62.9	0.88	3.19

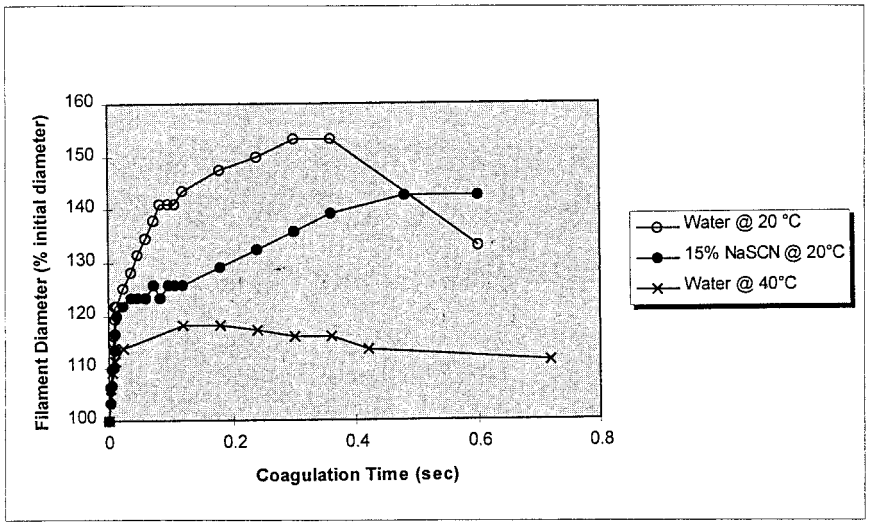

Figure 2 Filament diameter change during coagulation (0–800 ms).

volume, as is the case for polymer blends, and thermally quenched polymer/solvent systems where the solvent is frozen, coarsening results ultimately in breakdown of the structure, but with retention of both phases. It is conjectured that in the case of a liquid nonsolvent-induced phase separation, where there is a route for transport away of the polymer lean liquid phase (i.e., into the precipitation bath), coarsening of the polymer phase results in volume reduction by loss of the polymer lean liquid. Such a mechanism could account for the observation of syneresis, the expression of liquid at the surface(s) of cast membranes, reported by researchers working in this field.[8]

At this point, it is worth referring to an effect noted further downstream in an acrylic wet spinning process, associated with the reduction in porosity of a formed filament during hot stretching. It has been suggested by the authors[9] that this could be a coarsening process, whose rate significantly increases above the wet (water-plasticized) T_g of PAN. The coarsening seen here will also be

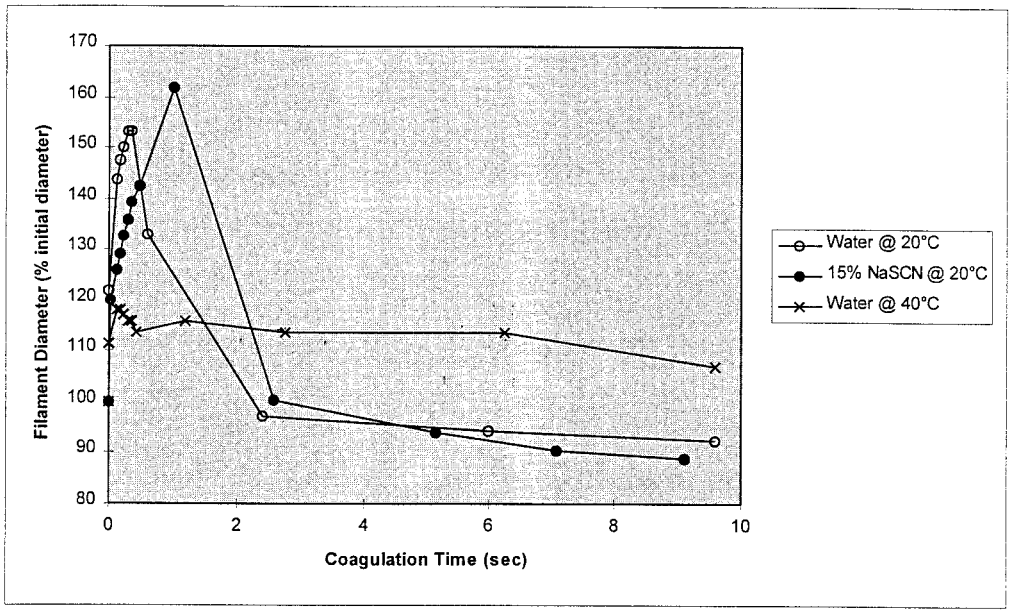

Figure 3 Filament diameter change during coagulation (0–10 s).

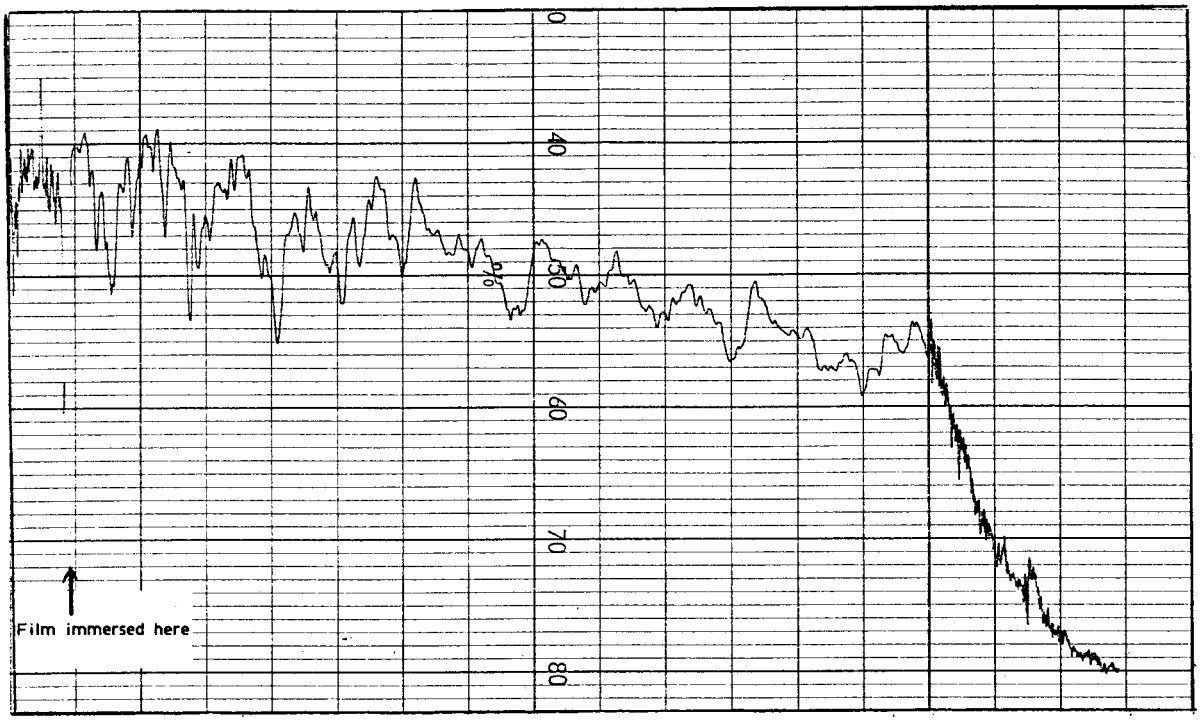

Figure 4 Light transmission trace for 1-mm film. Coagulant water at 20°C.

linked to the mobility of the polymer phase through the T_g, which will, in turn, be changing with the solvent content during coagulation. Once the T_g of the filament falls below the system temperature, coarsening will be significantly arrested. This scheme qualitatively fits the data summarized in Figure 3.

Kinetics of Coagulation

Judging by the extensive upheaval in the composition of the coagulating filament, phase separation will be occurring at some point during these changes. It is widely recognized now that two modes of liquid/liquid phase separation can occur in these ternary systems.[10] One is when demixing occurs immediately at the top surface on immersion into the nonsolvent, so-called instantaneous, and a second when there is a delay in demixing while diffusional exchange takes place throughout the thickness of the polymer solution to move the composition at the surface into the demixing region. Light transmission experiments can be used to determine which mode is in operation.

If the delay time is very short, it cannot be discerned from a typical light transmission trace. Since it has been found that the delay time in these systems is proportional to the square of the thickness of polymer solution,[11] the delay time can be easily increased by precipitating thick films. Consequently, coagulations were carried out with 1000-μm-thick films to ascertain the mode of demixing. Figure 4 shows a light transmission trace for an initially 1000-μm-thick film precipitated in water at 20°C. The trace is "noisy" due to refractive index changes in the bath as the higher density sodium thiocyanate leaves the film and falls to the base of the bath. Additionally, the magnitude of light attenuation as a result of the appearance of discontinuities in the film is fairly small. However, it can be seen that demixing occurs instantaneously upon immersion into the bath.

An equivalent trace is shown in Figure 5 for the precipitation of a 1000-μm film in water at 40°C. Under these conditions, the film is far more opaque after demixing so the attenuation of light is more pronounced. Again, instantaneous demixing is the mode of phase separation.

Figure 6 shows a trace for a 1000-μm film precipitated in 15% NaSCN at 20°C. Light attenuation due to demixing is low as films coagulated under these conditions are quite clear. However, it is possible to be fairly certain that demixing occurs instantaneously.

A second feature of these data is the possibility

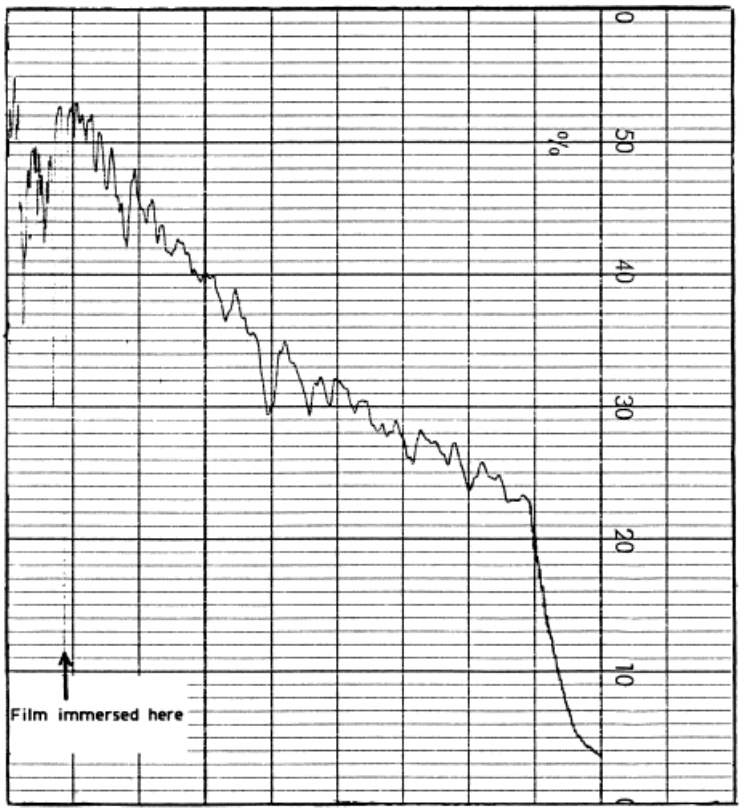

Figure 5 Light transmission trace for 1-mm film. Coagulant water at 40°C.

of extracting the time for demixing to take place through the thickness of the film. This is crudely taken as the time from immersion to the point at which no further attenuation of light is measured. To compute this and relate the times to the fiber-spinning case, film samples the thickness of half the diameter of the die-swollen filaments have to be analyzed (about 65 μm). Unfortunately, it was found at low film thickness that the "noise" due to Schleiren lines caused by inadequate solvent/bath mixing masked the very small change in clarity of these thin films. Even introducing stirring did not clear the problem. Hence, the video technique was developed, which proved to be insensitive to bath refractive index changes as the camera focuses directly onto the film. With a data acquisition rate of one frame every 40 ms, a number of snapshots of the film can be taken while coagulation takes place.

Figure 7 shows the change in the gray scale number as a function of time for coagulation of 64-μm films in water at 20 and 40°C and in 15% NaSCN at 20°C. Here, a higher gray scale value represents a whiter (less clear) image. In the first instance, it is clear that phase separation occurs instantaneously in each case, as suggested by the light transmission data on thick films. It is also clear that the bulk of phase separation has been completed within a second. This coincides roughly with the timescale at which filament swelling as a result of ingress of the nonsolvent is complete, before coarsening sets in and reduces the filament diameter. The fact that the time for complete phase separation of the film coagulated into 15% NaSCN is greater than the coagulation in water also fits the filament diameter data where coarsening begins at a later time. This is expected since the driving force for phase separation in a coagulant containing an amount of solvent will be reduced. The major conclusion from these kinetic data is that coarsening does appear to set in after phase separation is roughly complete.

At the outset, this study was designed to produce the average composition of an acrylic filament as it precipitates in a nonsolvent in order to plot its course traversing the phase diagram. This course is now plotted on the ternary phase diagram for the PAN/NaSCN/water system produced in a previous publication of the authors,[1] shown in Figure 8 for the three cases of precipita-

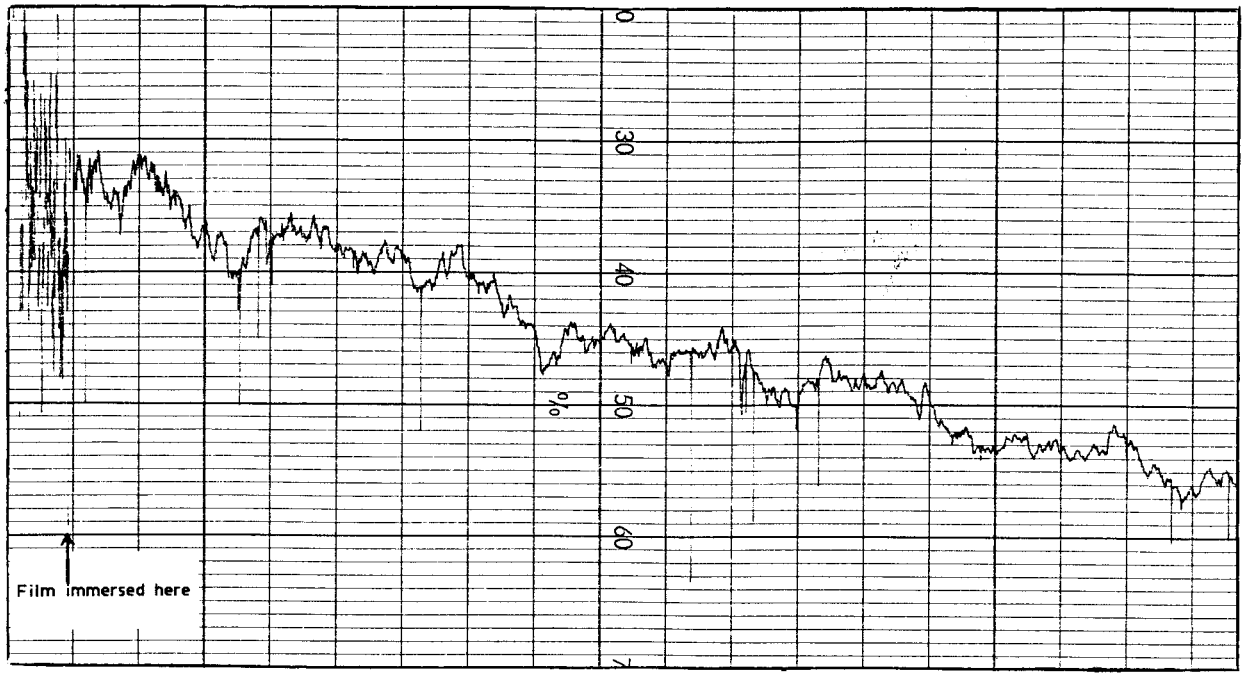

Figure 6 Light transmission trace for 1-mm film. Coagulant 15% NaSCN at 20°C.

tion into water at 20 and 40°C and into 15% NaSCN at 20°C. It was found in previous work that there was a negligible effect of temperature on the location of the binodal between 20 and 40°C, so a single curve is shown here.

Because of the unexpected coarsening of the structure artificially increasing the measured polymer concentration, the points at later timescales are not a reliable indicator of the demixing process. However, a number of salient features can be observed. It should be reiterated that the trajectories plotted represent average compositions. In reality, the nature of precipitation by a liquid nonsolvent means that changes begin at the filament exterior surface and composition gradients will be set up radially. The resulting structural asymmetry has long been a feature of certain types of membranes and has been reported extensively.[2] The polymer concentration at which the average composition crosses the binodal will

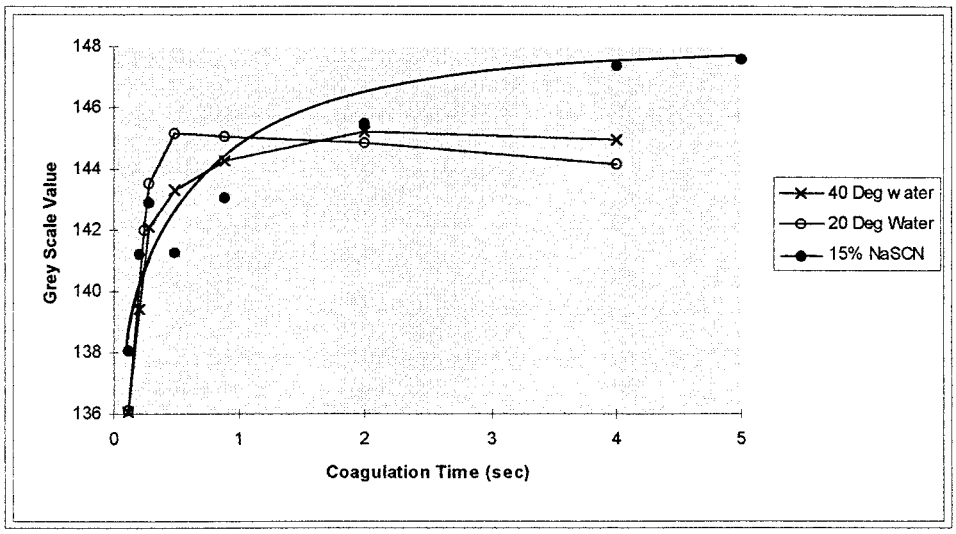

Figure 7 Gray scale number of film versus coagulation time.

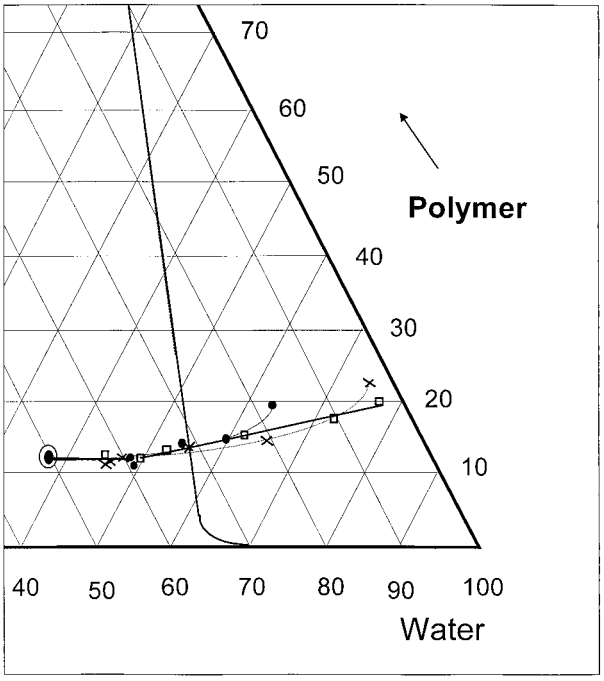

Figure 8 Phase diagram for PAN/NaSCN/water showing compositional trajectories: (●----) water at 40°C; (X-·-·-) water at 20°C; (□ ——) 15 % NaSCN at 20°C.

tend to dictate the level of porosity of the resulting solid phase.[12,13] The trajectories shown here appear to cross the binodal in a narrow range of around 12–14% polymer with little distinction between coagulation conditions. It was shown previously for this system that increasing the coagulation temperature serves to increase the porosity, with an increase from 20 to 40°C increasing the imbibed water level from about 280% to about 380%.[1] It might therefore be expected that coagulation into water at 40°C might result in crossing the binodal at a lower polymer content, but this is not evident from Figure 8. However, the level of porosity expected from the phase diagram as determined from the Lever Rule is around 330 and 400% for precipitation at 20 and 40°C, respectively, satisfyingly in accord with the imbibed water values found in the previous study. Note that tie lines have not been produced for this system, but it is likely that near to the PAN/water axis tie lines more or less follow the axis and the polymer will be essentially absent from the polymer lean phase. This allows an estimation of the relative amount of each phase at the end points of the trajectories in Figure 8 from the Lever Rule. The basis for this is inference from a previous study by Altena and Smolders on the effect of interaction parameters on the phase diagram in similar ternary systems.[14]

CONCLUSIONS

In a typical commercial process that produces acrylic fibers, a solution of a PAN terpolymer in aqueous sodium thiocyanate is extruded into an aqueous bath. The composition of a spinning filament has been measured gravimetrically at various times during its formation. In each of three precipitant baths (water at 20 and 40°C and 15% NaSCN at 20°C), ingress of water at a greater rate than egress of the solvent was observed at short timescales (<4 s). After this, both the solvent and nonsolvent appeared to leave the filament.

Measurement of the filament diameter by photomicroscopy during spinning revealed that the filament first grew beyond the die-swollen diameter, then at later times reduced in size, corroborating the compositional data. A polymer-coarsening mechanism was proposed to explain this phenomenon, whereby the polymer lean phase is effectively squeezed out from the matrix, with a concomitant reduction in volume.

The kinetics of phase separation have been studied using a light-transmission technique applied to the polymer solution in the film geometry. This showed that for the three precipitation conditions, phase separation was instantaneous. To measure the time taken for phase separation to be complete, a video technique was developed, whereby a video camera records the coagulation process of a film, allowing digitization of the sequence frame by frame and the assignment of a gray scale value to monitor the opacity of the coagulating film. Phase separation was shown to be largely complete within a second, which reasonably coincides with the compositional changes taking place. Coarsening of this newly formed two-phase structure would seem a reasonable explanation for the subsequent reduction in the filament diameter and apparent increase in the polymer concentration. When the compositional data are plotted as trajectories on the phase diagram for the system, points beyond the binodal at longer timescales should be treated with care, as they reflect the polymer-coarsening effect.

The authors thank Jason Yorke and Steve Smith at Courtaulds Corporate Technology for the video work

and for valuable discussions, respectively. The authors also thank Courtaulds plc for supporting this work.

REFERENCES

1. S. J. Law and S. K. Mukhopadhyay, *J. Appl. Polym. Sci.,* **65,** 2131–2137.
2. M. Mulder, *Basic Principles of Membrane Technology,* Kluwer, Dordrecht, The Netherlands, 1991.
3. A. J. Reuvers and C. A. Smolders, *J. Membr. Sci.,* **34,** 67 (1987).
4. L. P. McMaster, *Aspects of Liquid–Liquid Phase Transition Phenomena in Multicomponent Polymeric Systems,* Advances in Chemistry Series, 142, American Chemical Society, Washington, DC, 1975.
5. G. T. Caneba and D. S. Soong, *Macromolecules,* **18,** 2545 (1985).
6. F.-J. Tsai and J. M. Torkelson, *Macromolecules,* **23,** 775 (1990).
7. J. H. Aubert, *Macromolecules,* **23,** 1446 (1990).
8. R. E. Kesting, *Synthetic Polymeric Membranes,* 2nd ed., Wiley, New York, 1985.
9. S. J. Law and S. J. Mukhopadhyay, to appear.
10. A. J. Reuvers, PhD Thesis, University of Twente, Enschede, The Netherlands, 1987.
11. A. J. Reuvers, J. H. A. van den Berg, and C. A. Smolders, *J. Membr. Sci.,* **34,** 45 (1987).
12. A. J. Reuvers and C. A. Smolders, *J. Membr. Sci.,* **34,** 67 (1987).
13. C. S. Tsay and A. J. McHugh, *J. Polym. Sci. Part B. Polym. Phys.,* **30,** 309 (1992).
14. F. W. Altena and C. A. Smolders, *Macromolecules,* **15,** 1491 (1982).